Nuclear photoabsorption at photon energies between 300 and 850 MeV

Michihiro Hirata,* Nobuhiko Katagiri, and Kazuyuki Ochi
Department of Physics, Hiroshima University, Higashi-Hiroshima 739, Japan

Takashi Takaki†
Onomichi University, Onomichi 722-002, Japan
(Received 3 January 2002; published 17 July 2002)

We construct the formula for the photonuclear total absorption cross section using the projection method and the unitarity relation. Our treatment is very effective when interference effects in the absorption processes on a nucleon are strong. The disappearance of the peak around the position of the D_{13} resonance in the nuclear photoabsorption can be explained with the cooperative effect of the interference in two-pion production processes, the Fermi motion, the collision broadenings of Δ and N^*, and the pion distortion in the nuclear medium. The change of the interference effect by the medium plays an important role.

DOI: 10.1103/PhysRevC.66.014612 PACS number(s): 25.20.Dc, 25.20.Lj, 14.20.Gk, 24.30.Gd

I. INTRODUCTION

The total photonuclear absorption cross section has been measured over broad mass number and in the energy range 300–1200 MeV at Franscati [1–3]. Especially, it was noted that the excitation peaks around the position of the D_{13} (1520 MeV) and F_{15} (1680 MeV) resonances disappear and above 600 MeV there is a strong reduction of the absolute value of the cross section per nucleon compared with the data for hydrogen [4,5] and deutron [6]. These experimental findings have been confirmed by the contemporary data on the photofission cross section of ^{238}U [7] and ^{235}U [8] obtained at Mainz up to 800 MeV. There were a couple of theoretical attempts to explain the strong reduction of the cross section [9–11]. It was necessary for them to assume large values for the collision widths of the D_{13} and F_{15} resonances to explain the above strong reduction [9,10]. However, it was pointed out in Ref. [11] that such significantly increasing resonance widths were hardly justified. These theoretical analyses must miss some important effects other than the collision broadening. In the previous paper we pointed out that the disappearance of the peaks around the position of the resonances higher than the Δ resonance in the nuclear photoabsorption can be explained with the cooperative effect of the interference in two-pion photoproduction processes, the collision broadenings of Δ and $N^*(1520)$, and the pion distortion in the nuclear medium [12]. Our finding means that the change of the interference effect by the medium plays an important role.

In this paper we present a formula for photonuclear total absorption cross sections based on the projection operator technique and apply our method to evaluate them in the extended energy region between 300 and 850 MeV. The experimental total absorption cross sections on a nucleon show that there is a fairly deep valley between the energy region of the Δ resonance and that of the N^* resonance. On the other hand, the experimental total cross sections on nuclei show that the above valley is almost filled up. Furthermore, it is very interesting to note that the mass number dependence of total cross sections quite vary with the photon energy as follows: $A^{0.8}$ around 300 MeV, $A^{1.7}$ around 500 MeV, and $A^{0.65}$ around 750 MeV. We will discuss whether the mass number dependence of total cross sections can be explained by our theoretical treatment and speculate what one can learn from the comparison of our results with the data.

In Sec. II we derive the formula for total nuclear photoabsorption cross sections and in Sec. III, numerical results and discussions are given. Section IV contains our conclusions.

II. FORMALISM OF TOTAL NUCLEAR PHOTOABSORPTION CROSS SECTION

The total photoabsorption cross section is propotional to the imaginary part of the elastic Compton scattering T matrix $T_{\gamma\gamma}$:

$$\sigma_T = -\frac{2\Omega}{v}\mathrm{Im}T_{\gamma\gamma} \tag{1}$$

$$= i\frac{\Omega}{v}(T_{\gamma\gamma} - T^{+}_{\gamma\gamma}), \tag{2}$$

which is obtained from the unitarity relation. Here Ω is the normalization volume and v is the relative velocity between the photon and nucleus. We will use this relation to derive the formula of the total cross section. The expession for the T matrix $T_{\gamma\gamma}$ is constructed using the projection operator technique and focusing on the second resonance energy region where the $N^*(1520)$ resonance plays an important role and the two-pion photoproduction prevails in addition to the one-pion photoproduction. The $N^*(1520)$ resonance can decay into both the πN and $\pi\pi N$ channels, whose branching fractions are comparable, and its $\pi\pi N$ decay occurs through two dominant modes, i.e., $\pi\Delta$ and ρN. The two-pion photopro-

*Electronic address: hirata@theo.phys.sci.hiroshima-u.ac.jp
†Electronic address: takaki@onomichi-u.ac.jp

duction takes place mainly through the $\pi\Delta$ and ρN channels. So we include the N^*, $\pi\Delta$ and ρN intermediate states in our formalism explicitly.

Along the above lines, we introduce the projection operators to separate the nuclear Hilbert space into the following subspaces: the space of photon plus nuclear ground state (P_γ), the space of both one-pion plus nuclear ground state and one-pion plus nuclear one particle-hole states (P_1), the space of two-pion plus nuclear particle-hole states (P_2), the space of one N^* plus nuclear one-hole states (D_1), and the space of both $\pi\Delta$ plus nuclear one-hole states and ρ plus nuclear particle-hole states (D_2), respectively. The remaining space is eliminated and taken into account in an effective interaction. Using Eq. (2) and the projection operator technique, the total nuclear photoabsorption cross section can be obtained as

$$\sigma_T=\frac{\Omega}{v}\Big[\sum 2\pi\delta(E-H_{P_1P_1})|T_{P_1\gamma}|^2 + \sum 2\pi\delta(E-H_{P_2P_2})|T_{P_2\gamma}|^2+\Omega^+_{D_1\gamma}(-2\mathrm{Im}W^{(1)}_{sp}) \times\Omega_{D_1\gamma}+\Omega^+_{D_2\gamma}(-2\mathrm{Im}W^{(2)}_{sp})\Omega_{D_2\gamma}-\Delta_1-\Delta_2\Big]. \quad (3)$$

Here H is the total Hamitonian of the system and $H_{P_1P_1}=P_1HP_1$ and $H_{P_2P_2}=P_2HP_2$. The first and second terms correspond to the one-pion and two-pion photoproduction, respectively, and in this expression the T matrices $T_{P_1\gamma}$ and $T_{P_2\gamma}$ do not include the final state interaction. The third and fourth terms describe the genuine many-body absorption processes arising from the N^*, $\pi\Delta$ and ρN intermediate states. $\Omega_{D_1\gamma}$ and $\Omega_{D_2\gamma}$ are matrix elements of a wave operator and $W^{(1)}_{sp}$ and $W^{(2)}_{sp}$ are phenomenological one-body operators describing medium corrections in the D_1 and D_2 spaces. The terms Δ_1 and Δ_2 appear due to the introduction of the one-body operator $W^{(1)}_{sp}$ and are subtracted in order to avoid the double counting of the processes included in $W^{(1)}_{sp}$. A detailed derivation of Eq. (3) and definitions of the above matrix elements are given in the Appendix.

Now we turn to discuss how to practically evaluate the total cross section based on Eq. (3). Below the second resonance energy region, the contribution from Δ-hole states must be added to Eq. (3) and is treated in the same way as the N^* resonance. Actual calculations for it are described in the pages that follow. For the one-pion photoproduction, the T matrix is given in terms of the Δ and N^* resonant amplitudes described by the isobar model and the remaining background multipole amplitudes. We employ the model by Ochi *et al.* [16] for the two-pion photoproduction. For simplicity we use the Fermi gas model for a nucleus.

The cross section of one-pion photoproduction off a proton in the nuclear matter is given in the laboratory frame by

$$\sigma^\pi_p=\frac{1}{v}\frac{3Z}{8\pi(k^p_f)^3}\int_0^{k^p_f}d\vec{p}_1 \times\int\frac{d\vec{q}}{(2\pi)^3}\frac{d\vec{p}}{(2\pi)^3}(2\pi)^4\delta^4(k+p_1-q-p) \times\frac{1}{2}\sum_{\lambda,\nu,\nu'}\sum_{t_\pi,t_N}|\langle\vec{q}t_\pi\vec{p}\,\nu' t_N|T_{P_1\gamma}|\vec{k}\lambda\vec{p}_1\nu\rangle \times|^2\theta(|\vec{p}|-k^{t_N}_f)\frac{M^2}{2k2\omega_{\vec{q}}E_{\vec{p}_1}E_{\vec{p}}}, \quad (4)$$

$$T_{P_1\gamma}=T_{N^*}+T_\Delta+T_B, \quad (5)$$

where T_{N^*} and T_Δ represent the N^* and Δ resonance terms, respectively and T_B is the background term. $\vec{k}$, $\vec{p}_1$, $\vec{q}$, and $\vec{p}$ are the momenta of the incident photon, target proton, outgoing pion, and outgoing nucleon, respectively. $E_{\vec{p}_1}$, $\omega_{\vec{q}}$, and $E_{\vec{p}}$ are the energies of the target proton, outgoing pion, and outgoing nucleon, respectively. Z and v denote the proton number and the relative velocity between the photon and nucleus, respectively. $k^{t_N}_f$ is the Fermi momentum depending on the isospin quantum number t_N. The notation for all other spin-isospin quantum numbers are self-explanatory. The N^* resonance term is expressed as

$$T_{N^*}=F_{\pi NN^*}G_{N^*}(s)\tilde{F}^+_{\gamma PN^*}, \quad (6)$$

$$G_{N^*}(s)=\{\sqrt{s}-[M_{N^*}(s)+\delta M_{N^*}] +i(\Gamma_{N^*}(s)+\Gamma_{N^*sp})/2\}^{-1}, \quad (7)$$

where $\sqrt{s}$ is the total center of mass energy. M_{N^*} and Γ_{N^*} in the N^* propagator G_{N^*} are the mass and the free width of N^*, respectively, which are given so as to describe the energy dependence of the πN D_{13}-wave scattering amplitude and the branching ratios at the resonance energy. As the medium corrections, we introduce the mass shift δM_{N^*} and spreading width Γ_{N^*sp} due to the collisions between N^* and other nucleons. $\tilde{F}^+_{\gamma PN^*}$ and $F_{\pi NN^*}$ are the γPN^* and πNN^* vertex functions, respectively, of which detailed forms are given in Ref. [15], and the former operator corresponds to $F^+_{D_1\gamma}$ in Eq. (A21) which includes the vertex correction. The Δ resonance term T_Δ is written in a similar form with T_{N^*} but is important only at the low energy range less than 500 MeV. The effective $\gamma P\Delta$ coupling constant including the vertex correction is obtained by the same way used in the fixing of the γPN^* coupling constant. Here the Born term with the cutoff form factor employed in Ref. [23] is assumed as the background multipole amplitude. The Pauli blocking effect for the Δ decay into πN becomes non-negligible at low energies, since the probability of the nucleon being emitted with a small momentum increases compared with the energy region of the N^* resonance [24,25]. Thus we include the Fock term in the Δ propagator to modify the free Δ self-energy in addition to the collision width. The back-

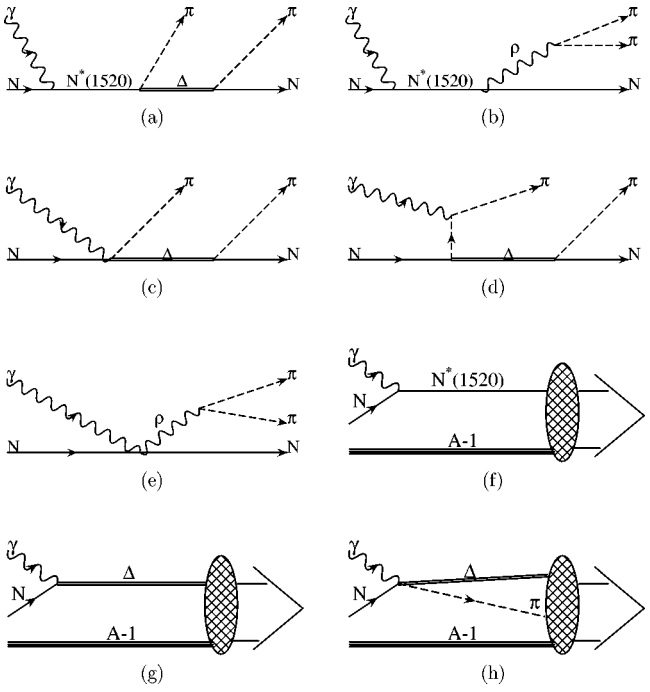

FIG. 1. Diagrams for the two-pion photoproduction on a nucleon and genuine many-body absorption processes on a nucleus. (a) The $N^* \to \pi\Delta$ contribution. (b) The $N^* \to \rho N$ contribution. (c) The Δ Kroll-Ruderman term. (d) The Δ pion-pole term. (e) The ρ Kroll-Ruderman term. (f) The many-body absorption process through the N^*. (g) The many-body absorption process through the Δ. (h) The many-body absorption process through the $\pi\Delta$. A is the mass number of the target nucleus.

ground amplitude T_B is evaluated by using the experimental multipole amplitudes [14]. We neglect medium corrections for the background amplitude, because its energy dependence is weak compared with the resonant amplitude and therefore the influence from these corrections to the total cross section is expected to be small. The integration over final particle momenta in Eq. (4) is performed by using variables defined in the γN center of mass system. We are interested in the absolute values of total nuclear photoabsorption cross sections. To investigate its damping effect, we need a model which gives a good description of two-pion photoproduction on nucleon. We use a simple model of Ochi *et al.* [16] where the total cross sections of its elementary processes are fairly reproduced as shown in Sec. III by taking into account the processes of Figs. 1(a)–(e). For simplicity, other possible diagrams obtained from the requirement of the gauge invariance and nonresonant background processes are neglected since these contributions are shown to be small [17]. Here we remark on the range parameter of the $\rho\pi\pi$ vertex function in the diagram (e). This range parameter was found to be rather small. Within our model, taking such a small value is only one way to fit the large cross section of $\gamma p \to \pi^+ \pi^0 n$. Its smallness may be related to the enhancement of the mass spectrum of the exchanged isovector $\pi\pi$ system, which is derived from the $N\bar{N} \to \pi\pi$ p-wave amplitude, in the lower energy region below the ρ meson peak [16,26]. Although our model must be improved to incorporate such an effect from a more fundamental level, it could be still applied to nuclear reactions as far as the present purpose is concerned.

The cross section of the two-pion photoproduction off a proton is given by

$$\sigma_p^{2\pi} = \frac{1}{v}\frac{3Z}{8\pi(k_f^p)^3}\int_0^{k_f^p} d\vec{p}_1 \int \frac{d\vec{q}_1}{(2\pi)^3}\frac{d\vec{q}_2}{(2\pi)^3}\frac{d\vec{p}}{(2\pi)^3} \times (2\pi)^4 \delta^4(k+p_1-q_1-q_2-p)\frac{1}{2} \times \sum_{\lambda,\nu,\nu'} \sum_{t_{\pi_1} t_{\pi_2} t_N} |\langle \vec{q}_1 t_{\pi_1} \vec{q}_2 t_{\pi_2} \vec{p} t_N \nu' | T_{P_2\gamma} | \vec{k}\lambda \vec{p}_1 \nu\rangle|^2 \times \theta(|\vec{p}| - k_f^{t_N}) \frac{M^2}{2k2\omega_{\vec{q}_1} 2\omega_{\vec{q}_2} E_{\vec{p}_1} E_{\vec{p}}}, \tag{8}$$

where $\vec{q}_1$ and $\vec{q}_2$ are the momenta of the outgoing pions. The medium-modified $T_{P_2\gamma}$ matrix is expressed as

$$T_{P_2\gamma} = T_{\Delta KR} + T_{\Delta PP} + T^s_{N^*\pi\Delta} + T^d_{N^*\pi\Delta} + T_{\rho \mathrm{KR}} + T_{N^*\rho N}. \tag{9}$$

The Δ Kroll-Ruderman term is written as

$$T_{\Delta KR} = F_{\pi N\Delta} G_{\pi\Delta}(s,\vec{p}_\Delta) F^+_{\Delta KR}, \tag{10}$$

$$G_{\pi\Delta}(s,\vec{p}_\Delta) = \{\sqrt{s} - \omega_\pi(\vec{p}_\Delta) - [M_\Delta(s,\vec{p}_\Delta) + \delta M_\Delta] + i[\Gamma_\Delta(s,\vec{p}_\Delta) + \Gamma_{\Delta sp}]/2 - V_\pi(\vec{q}_\pi)\}^{-1}. \tag{11}$$

Here $F_{\pi N\Delta}$ is the $\pi N\Delta$ vertex function, and $F^+_{\Delta \mathrm{KR}}$ is the Δ Kroll-Ruderman vertex function. The detailed forms of vertex functions are given in Ref. [15]. $V_\pi(\vec{q}_\pi)$ is the pion self-energy due to the distortion. $\vec{p}_\Delta$ is the γN center of mass momentum of Δ and $\vec{q}_\pi$ is the outgoing pion momentum. M_Δ and Γ_Δ in the propagator $G_{\pi\Delta}$ are the mass and the free width of Δ, respectively, and δM_Δ and $\Gamma_{\Delta sp}$ are the mass shift and collision width, respectively. Here we assume that the one-body operator $W^{(2)}_{sp}$ is given by the sum of the pion optical potential and the Δ spreading potential. We neglect the medium correction for the ρ meson since it is far off shell. The other terms in the right-hand side of Eq. (9) and the correction term Δ_1 are expressed in a similar way. The detailed forms of free T matrices are given in Ref. [15].

In addition to the one- and two-pion photoproduction processes, there are three genuine many-body processes which are shown in Figs. 1(f)–(h). The cross section for Fig. 1(f) corresponds to the third term of Eq. (3) and is given by

$$\sigma^{p}_{N^*(A-1)} = \frac{1}{v}\frac{3Z}{8\pi(k_f^p)^3}\int_0^{k_f^p} d\vec{p}_1 \Gamma_{N^*sp}\frac{1}{2} \times \sum_{\lambda\nu\nu_{N^*}} |G_{N^*}(s)\langle \vec{p}_{N^*}\nu_{N^*}|\tilde{F}^{+}_{\gamma P N^*}|\vec{k}\lambda\vec{p}_1\nu\rangle|^2 \times \frac{1}{2k}\frac{M}{E_{\vec{p}_1}}. \quad (12)$$

The cross section for Fig. 1(g) has a similar form to Eq. (12). The cross section for Fig. 1(h) corresponds to the fourth term of Eq. (3) and is given by

$$\sigma^{p}_{\pi\Delta(A-1)} = \frac{1}{v}\frac{3Z}{8\pi(k_f^p)^3}\int_0^{k_f^p} d\vec{p}_1 \int \frac{d\vec{q}}{(2\pi)^3}\frac{d\vec{p}}{(2\pi)^3} \times [\Gamma_{\Delta sp} + 2\mathrm{Im}V_\pi(\vec{q})](2\pi)^3\delta(\vec{k}+\vec{p}_1-\vec{q}-\vec{p}) \times \frac{1}{2}\sum_{\lambda\nu\nu_\Delta} |G_{\pi\Delta}(s,p_\Delta)\langle \vec{q}t_\pi\vec{p}\nu_\Delta t_\Delta|F^{+}_{\gamma P\pi\Delta} \times |\vec{k}\lambda\vec{p}_1\nu\rangle|^2 \frac{1}{2k2\omega_{\vec{q}}}\frac{M}{E_{\vec{p}_1}}, \quad (13)$$

where $F^{+}_{\gamma P\pi\Delta}$ describes the $\gamma P\to\pi\Delta$ transition corresponding to Figs. 1(a)–(d). To evaluate the cross section of Eq. (13), one needs to know the momentum dependence of $\Gamma_{\Delta sp}$ and $\mathrm{Im}V_\pi(\vec{q})$. The width $\Gamma_{\Delta sp}$ is assumed to be constant in the kinematical region where the process $\Delta N\to NN$ occurs and zero outside this physical region. The second term related to $\mathrm{Im}V_\pi(\vec{q})$ describes the process that the Δ resonance decays into πN while the pion is absorbed by nucleus. In order to include this instability of the Δ, we replace $\mathrm{Im}V_\pi(q)$ with $\mathrm{Im}\tilde{V}_\pi(\vec{q},E_\Delta)$ which is written as

$$\mathrm{Im}\tilde{V}_\pi(\vec{q},E_\Delta) = \left(-\frac{1}{\pi}\mathrm{Im}\frac{1}{D(\sqrt{s_\Delta})}\right)\mathrm{Im}V_\pi(\vec{q},q_0), \quad (14)$$

where $s_\Delta = E_\Delta^2 - \vec{p}^2$ and $q_0 = k + E_{p_1} - E_\Delta$, respectively, and $D(\sqrt{s_\Delta})$ is the free D function of the Δ. Then the expression obtained is integrated over the Δ energy E_Δ in addition to momenta of $\vec{p}_1$, $\vec{q}$, and $\vec{p}$. Generally, the pion absorbed becomes off shell, but in our calculation we use the one-shell value at $s_{\pi N} = q_0^2 - \vec{q}^2$ for Im $V_\pi(\vec{q},q_0)$ as an approximation. The correction term Δ_2 in Eq. (3) is evaluated in the same way as Eq. (13). The cross sections of photoabsorption on a neutron in the nuclear matter are also given in a similar form with those of a proton.

III. NUMERICAL RESULTS AND DISCUSSIONS

Let us start from the comments for photoabsorption reaction off a nucleon because the information of the elementary pion productions is very important to understand the strong damping mechanism of the N^* resonance. The dominant reactions on a nucleon over the photon energies from 300 to 850 MeV are the one-pion and two-pion photoproduction [13]. At first it is noted that the peak of the N^* resonance energy region shows up clearly by the combined effect of one-pion and two-pion productions as shown in Figs. 2(a) and (b), where the cross section of one-pion production has a small peak around 720 MeV and the cross section of two-pion production starts to grow from 400 MeV and increases up to around 800 MeV. The cross section of one-pion production is calculated by using the amplitudes of Arndt *et al.* [14] and that of two-pion production is calculated by our model [15,16].

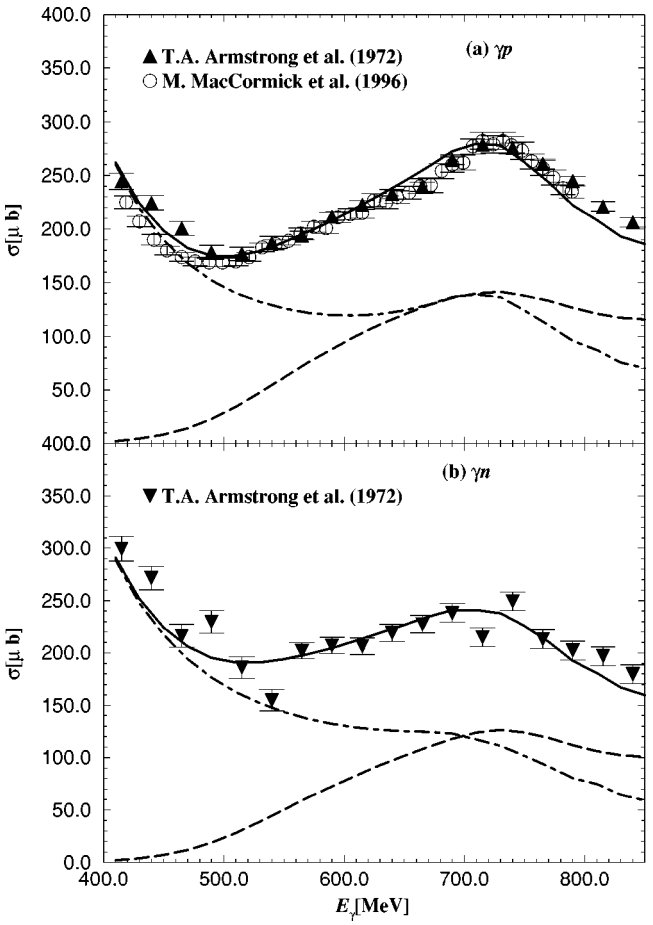

FIG. 2. The total photoabsorption cross sections on a proton and a neutron. The dash-dotted line is the contribution of the one-pion production obtained by using SM95 amplitudes of Arndt *et al.* [14]. The dashed line is the contribution of the two-pion production calculated by our model [15,16]. The solid line is the sum of those contributions. (a) Open circles and triangles (up) represent the data of total photoabsorption cross section on a proton [5,6]. (b) Triangles (down) represent the data of total photoabsorption cross section on a neutron [6].

We briefly review our model for the two-pion production. For the $\gamma N\to\pi^+\pi^- N$ reaction, four processes expressed by the diagrams Figs. 1(a)–(d) are assumed to contribute to this channel. In these processes, the Δ Kroll-Ruderman (ΔKR) term [Fig. 1(c)] and the Δ pion-pole (ΔPP) term [Fig. 1(d)] dominate on the cross section. The N^* contributions alone are small, but the interference among the N^* terms, the ΔKR

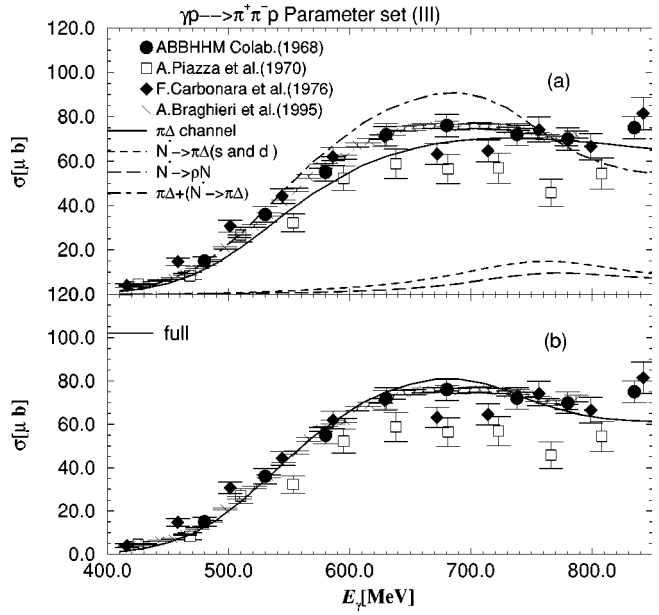

FIG. 3. The total cross section for the $\gamma p \rightarrow \pi^+ \pi^- p$. (a) The solid line is the contributions of the Δ Kroll-Ruderman and Δ pion-pole terms ($\pi\Delta$ channel), the dashed line is the contributions of the $N^* \rightarrow \pi\Delta$ (s- and d-wave) terms, the long dashed line is the contribution of the $N^* \rightarrow \rho N$ term, and the dash-dotted line is the sum of contributions from $\pi\Delta$ channel and $N^* \rightarrow \pi\Delta$ term. (b) The solid line corresponds to the full calculation. Theoretical lines are obtained by using the parameter set (III) in our model [16]. Experimental data are taken from Refs. [13,18–21].

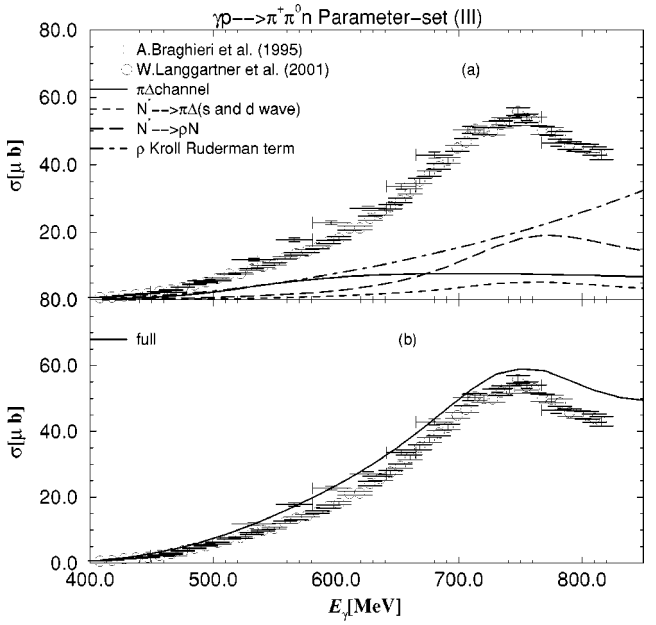

FIG. 4. The total cross section for the $\gamma p \rightarrow \pi^+ \pi^0 n$. (a) The solid line is the contribution of the Δ Kroll-Ruderman and Δ pion-pole terms ($\pi\Delta$ channel), the dashed line is the contribution of the $N^* \rightarrow \pi\Delta$ (s- and d-wave) terms, the long dashed line is the $N^* \rightarrow \rho N$ term, and the dash-dotted line is the contribution of ρ Kroll-Ruderman term. (b) The solid line corresponds to the full calculation. Theoretical lines are obtained by using the parameter set (III) in our model [16]. Experimental data are taken from Refs. [13,22].

and ΔPP terms is important as shown in Figs. 3(a) and (b). Because of this, the N^* excitation is regarded as an important ingredient in the two-pion photoproduction. For the $\gamma p \rightarrow \pi^+ \pi^0 n$ and $\gamma n \rightarrow \pi^- \pi^0 p$ reactions, the ρ meson Kroll-Ruderman (ρKR) term can contribute to these isospin channels in addition to four diagrams appearing in the $\gamma N \rightarrow \pi^+ \pi^- N$. The ρKR term [Fig. 1(e)] and the N^* terms dominate in this case, and the interference among the ρKR term, $N^*\rho$N term, and the ΔKR term is important and gives rise to the bump in the excitation curve as shown in Figs. 4(a) and (b). With regard to the $\gamma N \rightarrow \pi^0 \pi^0 N$ reaction, the magnitude of the cross section is underestimated about a factor of $\frac{3}{4}$ in our model. However, the underestimate of this channel does not affect our conclusion as far as the total cross section is concerned, since the cross section of $\gamma N \rightarrow \pi^0 \pi^0 N$ reaction is smaller than 10% of total two-pion production reaction.

What we learned from the elementary processes are the following.

(i) The cross section of one-pion photoproduction has only a small bump for a proton and a shoulder for a neutron in the N^* resonance energy region. Therefore we can easily make the N^* resonance peak from the one-pion production vanish by introducing a much smaller width due to the collision broadening than those given by Alberico *et al.* [9] and Kondratyuk *et al.* [10].

(ii) For the two-pion photoproduction the N^* contribution alone is not large. In order to give rise to the bump in the cross section, the interference between the N^* term and other terms is very important. So, we expect that the delicate balance of the interference is broken in the nuclear medium by the collision broadenings of Δ and N^*, the pion distortion in the $\pi\Delta$ channel and the Fermi motion, and therefore, the bump is strongly suppressed due to cooperative effects of the broadenings and interference.

Now we discuss the total cross section of nuclear photoabsorption. For simplicity we adopt the Fermi gas model for a nucleus, and $k^{av}{}_f = \int d\vec{r} \rho(\vec{r}) k_f(\rho)$ as the Fermi momentum in order to take into account the finiteness of nucleus. In our calculation, the total cross section per nucleon is obtained by taking the average of contributions from a proton and neutron in the nuclear matter.

As shown in Fig. 5, the Fermi motion produces strong damping of the cross section around the N^* resonance energy region. However, the small bump still remains and its effect cannot fill up the valley between 380 and 500 MeV. For comparison, we also show the experimental cross section on a free proton with the theoretical curve in Fig. 5. Furthermore, to see the details of the Fermi motion effects, individual contributions for the one-pion and two-pion productions are presented in Fig. 5. The size of the Pauli blocking effect for the intermediate and final states is found to be small but non-negligible as is seen from the difference between the dotted and thick solid lines.

To explain the data thus one inevitably needs the other damping mechanisms. As additional medium corrections, we take into account the spreading potentials [12] for the N^* and Δ resonances, and the pion distortion appearing in the

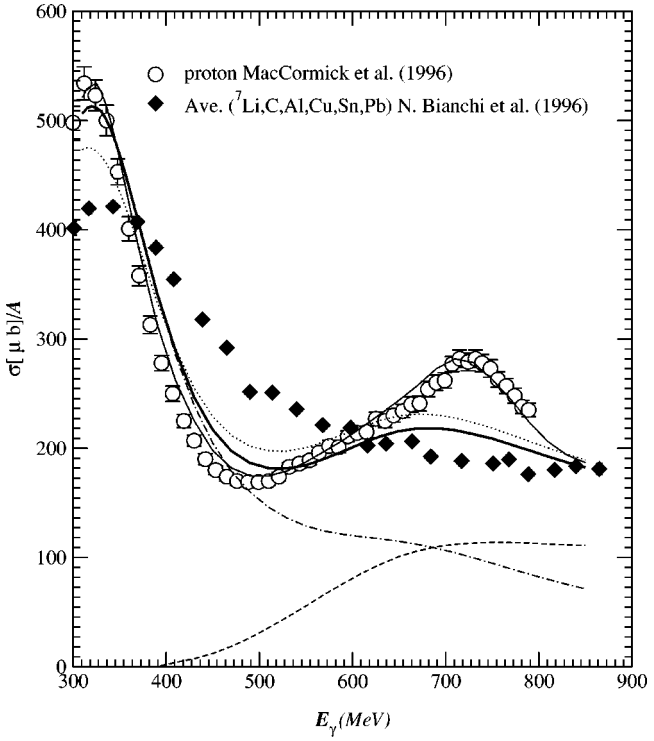

FIG. 5. The Fermi motion effects for total nuclear photoabsorption cross section on nuclei. The dotted line is the nuclear cross section averaged over the initial nucleon momentum. The thick solid line is the nuclear cross section including the Pauli blocking effect for the final emitted nucleon and intermediate Δ state in addition to the average over the initial nucleon momentum. The dash-dotted and dashed lines are two components of the thick solid line, i.e., the one-pion and two-pion production, respectively. The thin solid line corresponds to the cross section on a free proton calculated by using multipole amplitudes. Experimental data for nuclei are taken from Ref. [3]. The open circles represent data of the total photoabsorption cross section on a proton from Ref. [5].

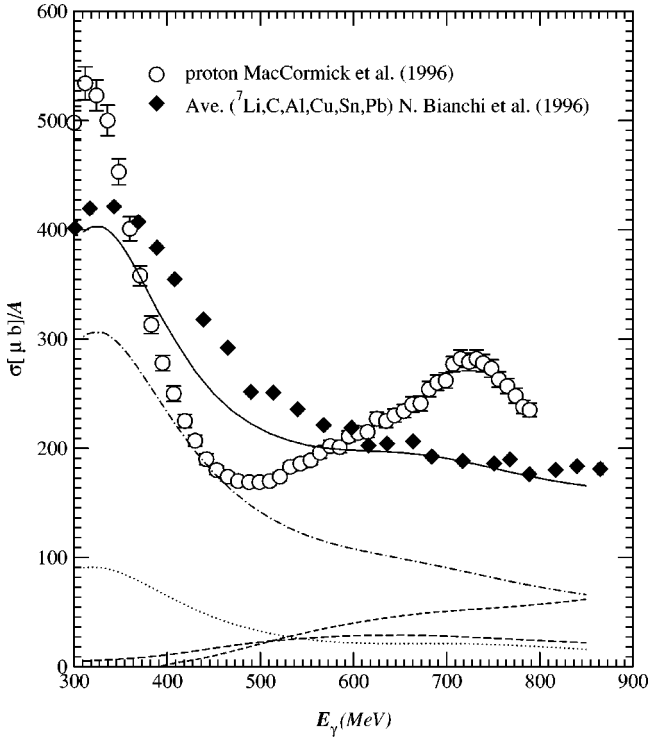

FIG. 6. The total nuclear photoabsorption cross section on nuclei. The solid line is the full calculation. The dash-dotted and dashed lines are the contributions of the one-pion and two-pion production, respectively. The dotted line is the contribution for the processes of Figs. 1(f) and (g). The long dashed line is the contribution for the process of Fig. 1(h). Experimental data for nuclei are taken from Ref. [3]. The open circles represent data of the total photoabsorption cross section on a proton from Ref. [5].

formula derived in the previous section. The mass shift and collision width of Δ have been already known in the studies of pion-nucleus scattering using the Δ-hole model [25,27–29] where they can be identified as the spreading potential. The spreading potential found in these studies is almost energy independent. We take $\delta M_\Delta = 6$ MeV and $\Gamma_{\Delta sp} = 36$ MeV. As the pion self-energy, we adopt the pion optical potential used by Arima *et al.* [30]. As for the mass shift and collision width of N^*, there are no established values at present. For simplicity, we assume that δM_{N*} and Γ_{N*sp} are energy independent like δM_Δ and $\Gamma_{\Delta sp}$. Then we vary the values so that the total nuclear photoabsorption cross sections from 600 to 800 MeV are reproduced. We found $\delta M_{N*} = 12$ MeV and $\Gamma_{N*sp} = 48$ MeV.

The total photoabsorption cross sections per nucleon (solid line) calculated with the above parameters are shown in Fig. 6. It is found that the simultaneus inclusion of the spreading potentials for the N^* and Δ resonances, and the pion distortion gives rise to the complete suppression of the bump around the N^* resonance energy region. To see the detailed contents of our calculations, furthermore, we show each contribution of the absorption processes: the one-pion production (dash-dotted line), the two-pion production (dashed line), the many-body absorption through the Δ-nucleus state and N^*-nucleus state (dotted line) corresponding to Figs. 1(f) and (g), and the many-body absorption through the $\pi\Delta$-nucleus state (long dashed line) corresponding to Fig. 1(h). The correction terms Δ_1 and Δ_2 in Eq. (3) are already included in the calculations of the dashed and long dashed lines, respectively. The size of the correction terms is small but non-negligible. For instance, there is about a 20% effect at 750 MeV for the two-pion production. In the one-pion photoproduction, the bump near the mass of the N^* disappears by the spreading potential for N^*. The cross section of the two-pion photoproduction is about three times smaller than that of the elementary process by the cooperative effects between the following medium corrections: the spreading potentials for Δ and N^*, the pion distortion, and the change of the interference among the related reaction processes. The cross sections of the other many-body processes are almost flat in the energy range above 600 MeV and small. As a consequence of these effects, the excitation peak around the position of the N^* resonance in the total nuclear photoabsorption cross section disappears differently from the hydrogen.

Our model, however, underestimates cross sections in the valley region between 380 and 500 MeV by about 15% ($\sim 45\mu$b). There must be some important processes which

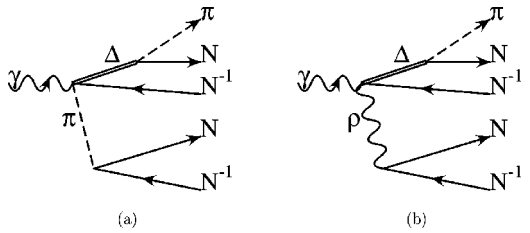

FIG. 7. The diagrams of two body contribution in the one-pion production.

give enhancement for the nuclear photoabsorption in the valley region but do not appear in the photoabsorption off a nucleon. The candidates for such processes are shown in Figs. 7(a) and (b) where the intermediate pion and ρ meson are far off shell. Two nucleons explicitly contribute to these processes and their short range correlation may be important. These contributions are suitable to explain the mass number dependence $A^{1.7}$ of total cross section in the valley region. In Refs. [11,31] the contribution from Fig. 7(a) is taken into account to increase the cross section of one-pion production.

The cross sections are also underestimated slightly at the Δ resonance energy around 320 MeV. This missing strength may be due to the coherent π^0 production mechanism in addition to the above two-nucleon mechanism. The coherent π^0 production is not included in our calculation using the Fermi gas model. In this energy region, our model has to be extended so as to treat the finiteness of the nucleus more reliably, as was done by Koch *et al.* [24].

IV. CONCLUSIONS

The formula derived by using the projection method for the photonuclear total absorption cross section has been presented. Our method is very effective for the case that the interference effect in the photoabsorption off a nucleon such as two-pion productions is strong.

The disappearance of the peak around the position of the D_{13} resonance in the nuclear photoabsorption can be explained by taking into account the cooperative effect of the interference in the two-pion photoproduction processes, the collision broadening of Δ and N^*, and the pion distortion in the nuclear medium. The change of the interference by the medium plays an important role. The mass shift and collision width of N^* are found to be $\delta M_{N^*}=12$ MeV and $\Gamma_{N^*sp}=48$ MeV, respectively. The collision width obtained is about six times smaller than those in Refs. [9,10]. The total absorption cross sections in our theoretical calculation around 320 MeV are about 5% smaller than average experimental cross sections for several nuclei. Furthermore, theoretical total absorption cross sections in the valley region between 380 and 500 MeV are about 15% smaller than the average experimental cross sections. In this energy region it may be necessary to take into account such reaction processes as Figs. 7(a) and (b) involving two nucleons explicitly.

APPENDIX: DERIVATION OF TOTAL NUCLEAR PHOTOABSORPTION CROSS SECTION

We give a derivation of total nuclear photoabsorption cross section by using the unitarity relation and the projection operator technique.

In order to simplify the formulation, we turn off the background interactions except the D_{13} channel in the one-pion production process, which will be later added in the formalism. We use the following projection operators to separate the nuclear Hilbert space into subspaces:

$$P_\gamma + p + q = 1. \tag{A1}$$

P_γ projects onto the space of photon plus nuclear ground state, p onto the spaces of both nuclear ground state and nuclear one particle-hole states except the P_γ space, and q onto the space of nuclear many particle-hole states. We assume that P_γ and q do not couple directly, i.e., $H_{\gamma q}=P_\gamma H q=0$, and neglect higher order terms of photocoupling. Here H is the total Hamiltonian of the system. Under such assumptions, the elastic compton scattering T matix becomes

$$T_{\gamma\gamma}=H_{\gamma p}\frac{1}{E-\mathcal{H}_{pp}}H_{p\gamma}, \tag{A2}$$

with

$$\mathcal{H}=H+H\frac{q}{E-H_{qq}}H, \tag{A3}$$

where $\mathcal{H}_{pp}=p\mathcal{H}p$ and $H_{qq}=qHq$, and E is the total energy of the system. The effective Hamiltonian $\mathcal{H}$ is introduced so as to eliminate the q space. The p space is further divided into the following spaces:

$$p=P+D, \tag{A4}$$

with

$$P=P_1+P_2, \tag{A5}$$

$$D=D_1+D_2, \tag{A6}$$

where P_1 projects onto the space of both one-pion plus nuclear ground state and one-pion plus nuclear one particle-hole states, P_2 onto the space of two-pion plus nuclear particle-hole states, D_1 onto the space of one N^* plus nuclear one-hole states and D_2 onto the spaces of both $\pi\Delta$ plus nuclear one-hole states, and ρ plus nuclear particle-hole states. Since $H_{\gamma q}=0$, then $\mathcal{H}_{\gamma P_1}=H_{\gamma P_1}$, $\mathcal{H}_{\gamma D_1}=H_{\gamma D_1}$, and $\mathcal{H}_{\gamma D_2}=H_{\gamma D_2}$. Unlike the Δ-hole model in the pion-nucleus scattering, the D_1 space is not a doorway between the subspaces P_γ and P_1+D_2, since the direct couplings described by $H_{\gamma P_1}$ and $H_{\gamma D_2}$ are non-negligible. $H_{\gamma P_1}$ corresponds to the background term in the D_{13} channel and $H_{\gamma D_2}$ corresponds to the Δ and ρ Kroll-Ruderman terms. This fact reflects the structure of the elastic compton scattering T matrix which will be shown later. To simplify the evaluation of the

T matrix of Eq. (A2), we must make some approximations for the reaction mechanism of the two-pion production: (1) P_γ and P_2 does not couple directly, i.e., $H_{\gamma P_2}=0$, so that $\mathcal{H}_{\gamma P_2}=0$. (ii) The transition between the space of P_1+D_1 and the space of P_2+D_2 proceeds only from the direct coupling of D_1 and D_2, so that $\mathcal{H}_{P_1P_2}=\mathcal{H}_{P_1D_2}=\mathcal{H}_{P_2D_1}=0$, and $\mathcal{H}_{D_1D_2}=H_{D_1D_2}$. In this way, we assume that the D_2 space plays the role of the doorway to two-pion states.

Inserting the projection operators of Eqs. (A4)–(A6) into Eq. (A2) and using the above-mentioned approximations, we obtain the elastic compton scattering T matrix given by

$$T_{\gamma\gamma}=T^{\gamma\gamma}_{P_1}+T^{\gamma\gamma}_{D_1}+T^{\gamma\gamma}_{D_2}, \tag{A7}$$

with

$$T^{\gamma\gamma}_{P_1}=H_{\gamma P_1}G_{P_1}H_{P_1\gamma}, \tag{A8}$$

$$T^{\gamma\gamma}_{D_1}=\tilde{F}_{\gamma D_1}G_{D_1}F^{+}_{D_1\gamma}, \tag{A9}$$

$$T^{\gamma\gamma}_{D_2}=H_{\gamma D_2}G_{D_2}H_{D_2\gamma}. \tag{A10}$$

The Green's functions in Eqs. (A8)–(A10) are defined as

$$G_{P_1}=(E-\mathcal{H}_{P_1P_1})^{-1}, \tag{A11}$$

$$G_{D_2}=(E-H_{D_2D_2}-H_{D_2P_2}G^0_{P_2}H_{P_2D_2}-\Sigma_{D_2})^{-1}, \tag{A12}$$

$$G_{D_1}=(E-H_{D_1D_1}-H_{D_1P_1}G^0_{P_1}H_{P_1D_1}-\Sigma_{D_1}-H_{D_1D_2}G_{D_2}H_{D_2D_1})^{-1}, \tag{A13}$$

where

$$\Sigma_{D_1}=H_{D_1q}\frac{1}{E-H_{qq}}H_{qD_1}+\mathcal{H}_{D_1P_1}G_{P_1}\mathcal{H}_{P_1D_1}-H_{D_1P_1}G^0_{P_1}H_{P_1D_1}, \tag{A14}$$

$$\Sigma_{D_2}=H_{D_2q}\frac{1}{E-H_{qq}}H_{qD_2}+\mathcal{H}_{D_2P_2}G_{P_2}\mathcal{H}_{P_2D_2}-H_{D_2P_2}G^0_{P_2}H_{P_2D_2}, \tag{A15}$$

and

$$G^0_{P_1}=(E-H_{P_1P_1})^{-1}, \tag{A16}$$

$$G^0_{P_2}=(E-H_{P_2P_2})^{-1}. \tag{A17}$$

The vertex functions in Eq. (A9) are defined as

$$F_{D_1\gamma}=H_{D_1\gamma}+\mathcal{H}_{D_1P_1}G_{P_1}H_{P_1\gamma}+H_{D_1D_2}G_{D_2}H_{D_2\gamma}, \tag{A18}$$

$$\tilde{F}_{\gamma D_1}=H_{\gamma D_1}+H_{\gamma P_1}G_{P_1}\mathcal{H}_{P_1D_1}+H_{\gamma D_2}G_{D_2}H_{D_2D_1}. \tag{A19}$$

In our formalism, the background coupling of P_γ and P_1 described by $H_{\gamma P_1}$ is included because the vertex correction of the second term in Eqs. (A18) and (A19) is known to be non-negligible in the elementary process. Since the strength of $H_{\gamma P_1}$ itself, however, is small, we neglect the process of $P_\gamma\rightarrow P_1\rightarrow q$. Thus Eq. (A8) is approximately written as

$$T^{\gamma\gamma}_{P_1}\cong H_{\gamma P_1}G^0_{P_1}H_{P_1\gamma}, \tag{A20}$$

and Eqs. (A18) and (A19) become

$$F^{+}_{D_1\gamma}\cong H_{D_1\gamma}+H_{D_1P_1}G^0_{P_1}H_{P_1\gamma}+H_{D_1D_2}G_{D_2}H_{D_2\gamma}, \tag{A21}$$

$$\tilde{F}_{\gamma D_1}\cong H_{\gamma D_1}+H_{\gamma P_1}G^0_{P_1}H_{P_1D_1}+H_{\gamma D_2}G_{D_2}H_{D_2D_1}. \tag{A22}$$

Hereafter, we use these approximate forms.

From Eq. (A7), we find the imaginary part of the T matrix:

$$T_{\gamma\gamma}-T^{+}_{\gamma\gamma}=T^{+}_{P_1\gamma}\Delta G^0_{P_1}T_{P_1\gamma}+T^{+}_{P_2\gamma}\Delta G^0_{P_2}T_{P_2\gamma}+\Omega^{+}_{D_1\gamma}(\Sigma_{D_1}-\Sigma^{+}_{D_1})\Omega_{D_1\gamma}+\Omega^{+}_{D_2\gamma}(\Sigma_{D_2}-\Sigma^{+}_{D_2})\Omega_{D_2\gamma}, \tag{A23}$$

with

$$\Omega_{D_1\gamma}=G_{D_1}F^{+}_{D_1\gamma}, \tag{A24}$$

$$\Omega_{D_2\gamma}=G_{D_2}(H_{D_2\gamma}+H_{D_2D_1}G_{D_1}F^{+}_{D_1\gamma}), \tag{A25}$$

and

$$T_{P_1\gamma}=H_{P_1\gamma}+H_{P_1D_1}\Omega_{D_1\gamma}, \tag{A26}$$

$$T_{P_2\gamma}=H_{P_2D_2}\Omega_{D_2\gamma}, \tag{A27}$$

where $\Delta G\equiv G-G^{+}$. T matrices of Eqs. (A26) and (A27) describe the one-pion photoproduction and two-pion photoproduction, respectively. The final state interactions, however, are not included in these expressions. Thus the cross sections calculated by Eqs. (A26) and (A27) do not exactly correspond to experimental cross sections. In our formalism, the effect of the final state interaction is contained in the third and fourth terms of Eq. (A23) and therefore there is an ambiguity in partitioning of the nuclear inelastic cross section. However, as far as total cross section is concerned, one can use Eq. (A23) to estimate it.

In the Green's function G_{D_2}, the operator $H_{D_2P_2}G^0_{P_2}H_{P_2D_2}$ is the free self-energies of the Δ and ρ meson corrected by the Pauli-blocking effect. In order to

clarify the physical content of operators in the Green's function G_{D_1}, we rewrite it as

$$G_{D_1}=(E-H_{D_1D_1}-H_{D_1P_1}G^0_{P_1}H_{P_1D_1} - H_{D_1D_2}G^0_{D_2}H_{D_2D_1}-\Sigma_{D_1}-\Sigma'_{D_1})^{-1}, \quad \text{(A28)}$$

where

$$\Sigma'_{D_1}=H_{D_1D_2}(G_{D_2}-G^0_{D_2})H_{D_2D_1}, \quad \text{(A29)}$$

and

$$G^0_{D_2}=(E-H_{D_2D_2}-H_{D_2P_2}G^0_{P_2}H_{P_2D_2})^{-1}. \quad \text{(A30)}$$

Here the operator $H_{D_1P_1}G^0_{P_1}H_{P_1D_1}$ consists of both the free N^* self-energy due to the one-pion channel corrected by the Pauli-blocking effect and the pion rescattering term arising from the coherent π^0 production. The operator $H_{D_1D_2}G^0_{D_2}H_{D_2D_1}$ corresponds to the free N^* self-energy due to the two-pion channel corrected by the Pauli-blocking effect. The self-energies $\Sigma_{D_1}+\Sigma'_{D_1}$ and Σ_{D_2} in Eqs. (A12) and (A28) are complicated many-body operators arising from the q-space coupling as well as the P_1- and P_2-spaces coupling. The latter coupling is related to the final state interaction in the one-pion or two-pion production. In practical calculations, these operators are assumed to be simple one-body operators,

$$\Sigma_{D_1}+\Sigma'_{D_1}\cong W^{(1)}_{sp}, \quad \text{(A31)}$$

$$\Sigma_{D_2}\cong W^{(2)}_{sp}, \quad \text{(A32)}$$

which are phenomenologically determined.

Using the expressions of Eq. (A23) with Eqs. (A31) and (A32), the total cross section can be written as

$$\sigma_T=\frac{\Omega}{v}\Big[\sum 2\pi\delta(E-H_{P_1P_1})|T_{P_1\gamma}|^2+\sum 2\pi\delta \times(E-H_{P_2P_2})|T_{P_2\gamma}|^2+\Omega^+_{D_1\gamma}(-2\mathrm{Im}W^{(1)}_{sp})\Omega_{D_1\gamma} +\Omega^+_{D_2\gamma}(-2\mathrm{Im}W^{(2)}_{sp})\Omega_{D_2\gamma}-\Delta_1-\Delta_2\Big], \quad \text{(A33)}$$

where

$$\Delta_1=\sum 2\pi\delta(E-H_{P_2P_2})|H_{P_2D_2}G_{D_2}H_{D_2D_1}\Omega_{D_1\gamma}|^2 - \sum 2\pi\delta(E-H_{P_2P_2})|H_{P_2D_2}G^0_{D_2}H_{D_2D_1}\Omega_{D_1\gamma}|^2, \quad \text{(A34)}$$

$$\Delta_2=\Omega^+_{D_1\gamma}H_{D_1D_2}G^+_{D_2}(-2\mathrm{Im}W^{(2)}_{sp})G_{D_2}H_{D_2D_1}\Omega_{D_1\gamma}. \quad \text{(A35)}$$

Here the terms Δ_1 and Δ_2 appear due to the introduction of the one-body operator $W^{(1)}_{sp}$ and are subtracted in order to avoid the double counting of the processes included in $W^{(1)}_{sp}$. Eq. (A33) is our starting point to calculate the total cross section. This equation shows that the absorption processes consist of three components, i.e., the quasifree processes such as the one-pion photoproduction and two-pion photoproduction, and genuine many-body absorption processes arising from the interaction between the resonance (or pion) and the nucleon in a nucleus [24]. In actual calculation, the Δ excitation and the remaining background processes except the D_{13} channel in the one-pion photoproduction must be added in the above formula.

[1] N. Bianchi *et al.*, Phys. Lett. B **229**, 219 (1993).
[2] M. Anghinolfi *et al.*, Phys. Rev. C **47**, R992 (1993).
[3] N. Bianchi *et al.*, Phys. Lett. B **309**, 5 (1993); **325**, 333 (1994); Phys. Rev. C **54**, 1688 (1996).
[4] T.A. Armstrong *et al.*, Phys. Rev. D **5**, 1640 (1972).
[5] M. MacCormick *et al.*, Phys. Rev. C **53**, 41 (1996).
[6] T.A. Armstrong *et al.*, Nucl. Phys. **B41**, 445 (1972).
[7] Th. Frommhold *et al.*, Phys. Lett. B **295**, 28 (1992).
[8] Th. Frommhold *et al.*, Z. Phys. A **350**, 249 (1994).
[9] W.M. Alberico, G. Gervino, and A. Lavagno, Phys. Lett. B **321**, 177 (1994).
[10] L.A. Kondratyuk *et al.*, Nucl. Phys. **A579**, 453 (1994).
[11] M. Effenberger, A. Hombach, S. Teis, and U. Mosel, Nucl. Phys. **A613**, 353 (1997).
[12] M. Hirata, K. Ochi, and T. Takaki, Phys. Rev. Lett. **80**, 5068 (1998).
[13] A. Braghieri *et al.*, Phys. Lett. B **363**, 46 (1995).
[14] R.A. Arndt, I.I. Strakovsky, and R.L. Workman, Phys. Rev. C **56**, 577 (1997), and references therein.
[15] K. Ochi, M. Hirata, and T. Takaki, Phys. Rev. C **56**, 1472 (1997).
[16] M. Hirata, K. Ochi, and T. Takaki, Prog. Theor. Phys. **100**, 681 (1998).
[17] J.A.G. Tejedor and E. Oset, Nucl. Phys. **A571**, 667 (1994); **A600**, 413 (1997).
[18] Aachen-Berlin-Bonn-Hamburg-Heidelberg-München Collaboration, Phys. Rev. **175**, 1669 (1968).
[19] A. Piazza *et al.*, Lett. Nuovo Cimento Soc. Ital. Fis. **3**, 403 (1970).
[20] F. Carbobara *et al.*, Nuovo Cimento A **36**, 219 (1976).
[21] A. Zabrodin *et al.*, Phys. Rev. C **55**, 1 (1997).
[22] W. Langgartner *et al.*, Phys. Rev. Lett. **87**, 052001 (2001).
[23] M. Betz and T.-S.H. Lee, Phys. Rev. C **23**, 375 (1981).
[24] J.H. Koch, E.J. Moniz, and N. Ohtsuka, Ann. Phys. (N.Y.) **154**, 99 (1984).
[25] M. Hirata, F. Lenz, and K. Yazaki, Ann. Phys. (N.Y.) **108**, 116 (1977).

[26] E. Oset, K. Toki, and W. Weise, Phys. Rep. **83**, 281 (1982).
[27] M. Hirata, J.H. Koch, F. Lenz, and E.J. Moniz, Ann. Phys. (N.Y.) **120**, 205 (1979).
[28] Y. Horikawa, F. Lenz, and M. Thies, Nucl. Phys. **A345**, 386 (1980).
[29] E. Oset and W. Weise, Nucl. Phys. **A319**, 477 (1979); **A329**, 365 (1979).
[30] M. Arima, K. Masutani, and R. Seki, Phys. Rev. C **51**, 285 (1995).
[31] R.C. Carrasco and E. Oset, Nucl. Phys. **A536**, 445 (1992).